



# Bifurcation in steady laminar mixed convection flow in uniformly heated inclined tubes

Bifurcation

543

J. Orfi and N. Galanis  
*Département de génie mécanique, Université de Sherbrooke,  
Sherbrooke, Québec, Canada and*

C.T. Nguyen  
*École de génie, Université de Moncton,  
Moncton, Nouveau-Brunswick, Canada*

Received March 1998  
Revised January 1999  
Accepted February 1999

**Keywords** *Laminar flow, Bifurcation, Tube*

**Abstract** *The fully developed laminar mixed convection flow in inclined tubes subject to axially and circumferentially uniform heat flux has been studied numerically for a Boussinesq fluid. Dual solutions characterized by a two- and a four-vortex secondary flow structure in a cross-section normal to the tube's longitudinal axis have been found for different combinations of the Grashof number  $Gr$  and of the tube inclination  $\alpha$  for all Prandtl numbers between 0.7 and 7. In the two-parameter space defined by  $Gr$  and  $\alpha$  dual solutions occur: at a given  $\alpha$ , if the Grashof number exceeds a critical value  $Gr_c$  (for horizontal tubes  $Gr_c$  is approximately  $5.5 \times 10^5$ ,  $1.7 \times 10^5$  and  $1.7 \times 10^4$  respectively for  $Pr = 0.7$ , 7 and 70); at a given  $Gr$ , if the tube inclination is below a critical value  $\alpha_c$  (for  $Gr = 10^6$  this critical angle is approximately  $62.5^\circ$  and  $83.5^\circ$  respectively for  $Pr = 0.7$  and 7). Numerical experiments carried out for developing flows indicate that the two-vortex solution is the only stable flow structure.*

## 1. Introduction

The problem of combined forced and free laminar convection in heated tubes has been the subject of many studies over the past decades since this flow situation is encountered in many engineering applications, such as solar collectors, pipelines and nuclear reactors. Under the effects of buoyancy, hot fluid rises along the tube wall and descends in the central part of the cross-section. This secondary motion destroys the symmetry of the primary axial flow. Thus, the resulting axial velocity profile is not parabolic and the isotherms are very different from the concentric circles corresponding to pure forced convection flow (Coutier, 1983). Furthermore, the Nusselt number and the friction coefficient depend on the Reynolds, Prandtl and Grashof numbers as well as on the tube inclination.

The characteristics of this complex flow field have been studied both experimentally and numerically. An extensive review of publications on this

---

The authors wish to thank the Natural Sciences and Engineering Research Council of Canada, the "Fonds FCAR du Québec" and the "Programme de Coopération Québec/Nouveau-Brunswick" for financial support for this project.

International Journal of Numerical  
Methods for Heat & Fluid Flow,  
Vol. 9 No. 5, 1999, pp. 543-567.  
© MCB University Press, 0961-5539

---

subject has been compiled by Kakac *et al.* (1987). Among the experimental investigations, the publications by Mori and Futagami (1967), Petukhov *et al.* (1967, 1969), Morcos (1974), Barozzi *et al.* (1985) and Bilodeau *et al.* (1997) present a description of the flow field as well as useful correlations for the axial evolution of the Nusselt number in terms of the Rayleigh number and for transition between the laminar and turbulent regimes. Early analytical studies used the perturbation technique (Morton, 1959), which is only valid for very small Rayleigh numbers. On the other hand, the boundary layer method used by Siegwarth (1968) seems to be appropriate only for relatively large Rayleigh numbers. Early numerical studies using the finite differences method were carried out by Newel and Bergles (1970) and by Collins (1971) for horizontal and vertical flows respectively. More recent projects using modern numerical algorithms and fast computers with extensive memory have investigated the characteristics of developing flows in isothermal tubes (Choudhury and Patankar, 1988) and in tubes with a uniform heat flux (Orfi *et al.*, 1997). They have also studied the effects of wall conduction in vertical (Heggs *et al.*, 1990) or inclined (Laouadi *et al.*, 1994) tubes, those of axial diffusion in low Peclet number flows (Wang *et al.*, 1994) as well as those of temperature dependent fluid properties (Nesreddine *et al.*, 1997).

Several investigators have observed the close similarity between the governing equations of the mixed convection flow in straight heated ducts and those for the Dean problem, i.e. laminar flow in a curved duct. The dynamic parameters for these two problems are, respectively, the Grashof and Dean numbers. In both cases, for small values of the dynamic parameters, the two-dimensional flow structure in a plane normal to the longitudinal axis of the duct consists of two symmetrical counter-rotating vortices. However, as the dynamic parameter increases, this two-cell flow structure becomes unstable and it eventually evolves into a four-cell structure. For a certain range of values of the dynamic parameters, the two flow structures coexist, that is the PDEs representing the flow field have two distinct solutions. Such a flow bifurcation for the Dean problem has been treated in detail by Nandakumar and Masliyah (1982), Winters (1987) and Bara *et al.* (1992). With regard to the mixed convection problem, Patankar *et al.* (1978) were probably the first to predict the transition from the two-cell to the four-cell structure for a Boussinesq fluid with  $Pr = 5$  in a horizontal non-uniformly heated circular tube. A similar transition was observed by Chou and Hwang (1984) for a uniformly heated rectangular duct. However, neither of these last two studies detected the existence of dual solutions. Choi and Choi (1992) re-examined Patankar's non-uniformly heated flow problem and established the existence of dual solutions for high values of the Grashof numbers and for all Prandtl numbers between 0.2 and 10.

For fully-developed laminar mixed convection in horizontal heated ducts, Nandakumar *et al.* (1985) have shown that bifurcation occurs beyond a critical Grashof number  $Gr_{\ell}$  in circular, semi-circular and rectangular geometries. In the case of the rectangular duct, they also found that the two-cell structure disappears when the Grashof number exceeds a second critical value  $Gr_u$

(where  $Gr_u > Gr_\ell$ ). Thus, for this particular geometry, the friction factor and the Nusselt number show a hysteresis behavior as the Grashof number is gradually increased and then decreased. The variation of the two critical Grashof numbers with the duct aspect ratio has a strong resemblance to the tilted cusp observed by Benjamin (1978a,b) and by Benjamin and Mullin (1982) in their studies of Taylor vortices. Recently, the bifurcation structure of the flow through a horizontal heated rectangular duct was re-examined in detail by Nandakumar and Weinitschke (1991). In addition to the primary branch with two limit points and a hysteresis behavior reported earlier, they obtained a much richer solution structure with up to five solutions (symmetric and asymmetric) over certain ranges of the Grashof number. For the case of the circular horizontal tube, the hysteresis behavior has not been established, probably because the second critical value  $Gr_u$  is higher than the range examined by Nandakumar *et al.* (1985). Furthermore, their results for this geometry indicate that the two- and four-vortex solutions correspond to very small differences in the values of the friction coefficient and of the Nusselt number.

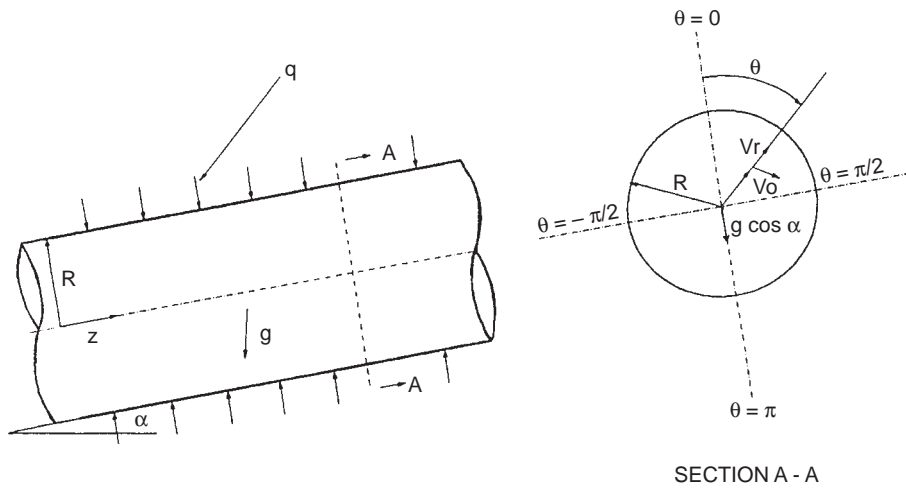
It is important to note that all the previously mentioned papers reporting the existence of two different flow structures for the mixed convection problem are concerned with horizontal ducts. Furthermore, the two papers by Nandakumar *et al.* (1985, 1991) which have studied the bifurcation structure of such flows have used the specific thermal boundary condition of a uniform heat flux in the axial direction and a uniform temperature around the duct's periphery. This condition corresponds to the case of ducts with low thermal resistance in the peripheral direction (thick walls and/or large ratios of wall-to-fluid conductivities). On the other hand, the present authors have considered inclined circular tubes with axially and circumferentially uniform heat flux (this condition corresponds to thin walls and/or small ratios of wall-to-fluid conductivities). They reported the existence of dual solutions for this problem and have compared the two- and four-cell structures for the flow of air for one particular combination of  $Re$ ,  $Gr$  and tube inclination (Orfi *et al.*, 1994).

In the present paper, the problem of bifurcation for fully-developed laminar mixed convection in inclined tubes with axially and circumferentially uniform heat flux at the solid-fluid interface is investigated thoroughly. The influence of the Grashof and Prandtl numbers as well as that of the tube inclination on the flow characteristics, the friction coefficient and the Nusselt number are presented and discussed. The state diagrams showing the domains of existence of dual solutions have also been determined.

## 2. Governing equations

We consider steady, laminar, fully-developed flow with combined forced and free convection within a straight tube of invariable circular cross-section inclined at an angle  $\alpha$  with respect to the horizontal. The fluid is subjected to a circumferentially and axially uniform heat flux  $q$  at the wall-fluid interface (Figure 1). The thermophysical properties of the fluid are assumed to be

**Figure 1.**  
Schematic  
representation of the  
geometry and coordinate  
system



constant except for the fluid density  $\rho'$  in the buoyancy force which is linearized as follows in terms of the temperature  $T'$ :

$$\rho' = \rho'_0 \left[ 1 - \beta_0 (T' - T'_0) \right] \quad (1)$$

Here  $\rho'_0, \beta_0$  are respectively the density and thermal expansion coefficient of the fluid corresponding to the fixed reference temperature  $T'_0$ .

The viscous dissipation is considered to be negligible and since the flow is assumed to be fully developed the following conditions prevail:

$$\frac{\partial \vec{V}'}{\partial Z} = 0 \quad \frac{\partial p'}{\partial Z} = \text{constant} \quad (2a)$$

and

$$\frac{\partial T'}{\partial Z} = \frac{dT'_m}{dZ} = \frac{2q}{\rho'_0 V'_m R C'_0} \quad (2b)$$

where  $\vec{V}'$  is the velocity vector,  $p'$  the pressure,  $C'_0$  the specific heat corresponding to  $T'_0$  and  $T'$ ,  $V'$  are respectively the fluid bulk temperature and its average axial velocity.

Furthermore, since the flow is assumed to be fully developed, the axial diffusion terms in the momentum equations are identically zero. Therefore, since conditions in one cross-section do not influence those in any other upstream one, the fluid pressure decomposition used extensively for axially parabolic flows (Patankar *et al.*, 1978; Bara *et al.*, 1992) can also be assumed to apply here:

$$p'(r', \theta, Z') = p'_1(r', \theta) + p'_2(Z') \quad (3)$$

where  $p'_1$  is the pressure variation around the cross-sectional average pressure  $p'_2$ . The validation of this approach is provided later by comparing calculated results with analytical solutions for pure forced flow and with experimental results for mixed convection. The following modified pressures are then introduced by combining  $p_1$  and  $p_2$  with the appropriate gravitational contributions:

$$P'_1 = p'_1 + \rho_0 r' g \cos \alpha \cos \theta \quad (4a)$$

$$P'_2 = p'_2 + g \sin \alpha \int_0^{Z'} \rho'_m dZ' \quad (4b)$$

where  $\rho'$  is the fluid density corresponding to the bulk temperature  $T'$ .

Next, the following dimensionless quantities are introduced:

$$r = \frac{r'}{D} \quad Z = \frac{Z'}{D \text{Re Pr}} \quad (5a)$$

$$V_r = \frac{V'_r D}{\alpha_0} \quad V_\theta = \frac{V'_\theta D}{\alpha_0} \quad V_z = \frac{V'_z}{V_m} \quad (5b)$$

$$T = \frac{T' - T_0}{qD/k_0} \quad P_1 = \frac{p'_1 D^2}{\rho_0 \alpha_0} \quad P_2 = \frac{p'_2}{\rho_0 V_m^2} \quad (5c)$$

With these definitions, the diffusion of heat in the axial direction is identically zero and the non-dimensional governing equations in cylindrical coordinates are:

$$\frac{\partial}{\partial r}(rV_r) + \frac{\partial V_\theta}{\partial \theta} = 0 \quad (6)$$

$$V_r \frac{\partial V_r}{\partial r} + \frac{V_\theta}{r} \frac{\partial V_r}{\partial \theta} = -\frac{\partial P_1}{\partial r} + \text{Pr} \nabla^2 V_r + S_r \quad (7)$$

$$V_r \frac{\partial V_\theta}{\partial r} + \frac{V_\theta}{r} \frac{\partial V_\theta}{\partial \theta} = -\frac{\partial P_1}{r \partial \theta} + \text{Pr} \nabla^2 V_\theta + S_\theta \quad (8)$$

$$V_r \frac{\partial V_z}{\partial r} + \frac{V_\theta}{r} \frac{\partial V_z}{\partial \theta} = -\frac{dP_2}{dZ} + \text{Pr} \nabla^2 V_z + S_z \quad (9)$$

$$V_r \frac{\partial T}{\partial r} + \frac{V_\theta}{r} \frac{\partial T}{\partial \theta} = \nabla^2 T \quad (10)$$

with

$$\nabla^2 = \frac{\partial^2}{\partial r^2} + \frac{1}{r} \frac{\partial}{\partial r} + \frac{1}{r^2} \frac{\partial^2}{\partial \theta^2} \quad (11)$$

The source terms in the momentum equations are:

$$S_r = \frac{V_\theta^2}{r} + Gr Pr^2 T \cos \alpha \cos \theta + Pr \left( -\frac{V_2}{r^2} - \frac{2}{r^2} \frac{\partial V_\theta}{\partial \theta} \right) \quad (12)$$

$$S_\theta = -\frac{V_r V_\theta}{r} - Gr Pr^2 T \cos \alpha \sin \theta + Pr \left( \frac{2}{r^2} \frac{\partial V_r}{\partial r} - \frac{V_\theta}{r^2} \right) \quad (13)$$

$$S_z = \frac{Gr Pr}{Re} T \sin \alpha \quad (14)$$

It can therefore be seen that the problem under study is characterized by four independent parameters, namely the Reynolds, Prandtl and Grashof numbers as well as the tube inclination  $\alpha$  with

$$Re = \frac{\rho_o V_m D}{\mu_o} \quad Pr = \frac{C_o \mu_o}{k_o} \quad (15a)$$

$$Gr = \frac{\rho_o^2 g \beta_o q D^4}{k_o \mu_o^2} \quad (15b)$$

Finally, the flow field is assumed to be symmetrical with respect to the vertical diameter. This assumption is supported by the experimental results of Mori and Futagami (1967) among others. It has been used to study fully developed mixed convection by Patankar *et al.* (1978) and Choi and Choi (1992) among others. It has also been used extensively for bifurcation studies of fully developed flow in curved ducts (Bara *et al.*, 1992 ; Nandakumar and Masliyah, 1982) and of fully developed mixed convection in horizontal ducts (Nandakumar *et al.*, 1985, 1991). It is of course true that this imposed symmetry does not allow the calculation of possible asymmetric solutions (such as those obtained by Winters (1987) for the Dean problem). However, it is believed that despite this limitation, the present study provides useful insights on bifurcation in inclined tubes for which no such results have been previously published to the best of our knowledge. In view of this assumption, only half of the circular cross-section needs to be considered. The following boundary conditions can then be specified:

- at the wall-fluid interface, the usual nonslip conditions prevail and the dimensionless radial gradient of the temperature is equal to unity to satisfy the condition of uniform heat flux:

$$\text{at } r = 0.5, \quad V_r = V_\theta = V_z = 0 \text{ and } \frac{\partial T}{\partial r} = 1 \quad (16a)$$

- along the vertical diameter the symmetry condition applies:

$$\text{at } \theta = 0 \text{ and } \theta = \pi, \quad V_\theta = 0 \text{ and } \frac{\partial V_r}{\partial \theta} = \frac{\partial V_z}{\partial \theta} = \frac{\partial T}{\partial \theta} = 0 \quad (16b)$$

In addition, the overall mass balance

$$\int_{z=0}^{0.5} \int_{\theta=0}^{\pi} V_z r d\theta dr = \frac{\pi}{8} \quad (17)$$

must be satisfied.

It is important to note that the axial gradient of the cross-sectional average pressure in equation (9) is, according to the assumption of fully-developed flow, a constant for a given set of values of the governing parameters Gr, Pr, Re and  $\alpha$ . However, its value remains unknown and must be computed as part of the solution.

### 3. Method and accuracy of solution

The numerical method employed to solve the coupled non-linear system of governing equations (6) through (10) subject to the boundary conditions expressed by equations (16) and (17) is based on the SIMPLE-C method (van Doormal and Raithby, 1984). The governing equations were discretized on staggered grids by integrating them over finite control volumes, using the power-law scheme (Patankar, 1980) to approximate the combined convective-diffusive terms. This integration process results in a system of algebraic equations which was successfully solved using the line-by-line technique (Patankar, 1980). The constant axial gradient of the cross-sectional average pressure is determined using an iterative procedure to satisfy the overall mass balance expressed by equation (17). In the present study, a trial-and-error secant-type method suggested by Laouadi *et al.* (1994) was adopted for the determination of the correct value of  $dP_2/dZ$ .

It should be noted that the singular point at  $r = 0$  does not pose any particular difficulties since, with the staggered grid used here, values of  $V_z$ , T and  $P_1$  are calculated at the center of the pie-shaped elements whose apex is at center of the cross-section. Furthermore, the radial velocity at  $r = 0$  does not contribute any fluxes since the corresponding area for these pie-shaped elements is zero.

Several different grids have been tested to ensure that the numerical results are independent of the number and distribution of the grid points employed in the discretization process. Using the average Nusselt number as the basis for comparisons, a grid with 36 and 32 points along the circumferential and radial

directions respectively was finally adopted (see Table I and Orfi (1995) for additional details). Along the radial direction, the spacing is non-uniform with grid lines highly packed near the wall.

In order to validate the model and the solution procedure, the computer program was first used to simulate pure forced flow (i.e.  $Gr = 0$ ). Results for the axial velocity and temperature profiles were in excellent agreement with the corresponding analytical solutions. The relative difference between the computed and analytical values of the average Nusselt number was less than 0.1 percent (Orfi, 1995). Furthermore, some calculated results for mixed convection within horizontal and vertical tubes have been compared with previously published values. Table II shows such a comparison for the calculated Nusselt number for air and water and three different Grashof numbers. The present results are within  $\pm 5$  percent of Van Dyke's values (1990) for horizontal tubes and within  $\pm 4$  percent of Petukhov *et al.* (1969) values for vertical tubes. In view of these results we conclude that the assumptions used to formulate the mathematical model are valid and that the numerical method is reliable.

#### 4. Results and discussion

All the results presented in this paper were calculated for  $Re = 500$  while the three other independent parameters ( $Gr$ ,  $Pr$  and tube inclination  $\alpha$ ) were varied. As stated previously, mixed convection in a straight tube constitutes a dissipative dynamic system for which the control, or forcing, parameter is the Grashof number. At low values of the latter, a typical flow structure in a cross-section normal to the longitudinal axis of the tube consists of two symmetrical

**Table I.**  
 Grid sensitivity  
 analysis for  $Pr = 7$  and  
 $\alpha = 0^\circ$

Grid	$Gr = 5 \times 10^4$ (2 cells)	$Gr = 2.5 \times 10^5$ (4 cells)	$Gr = 10^6$ (4 cells)	Lower critical Grashof number
$16 \times 16$	7.94	9.70	11.43	$7.5 \times 10^4 < Gr_\ell < 10^5$
$28 \times 24$	7.80	9.43	10.95	$10^5 < Gr_\ell < 2.5 \times 10^5$
$36 \times 32$	7.76	9.35	10.81	$10^5 < Gr_\ell < 2.5 \times 10^5$

**Table II.**  
 Comparison of the  
 calculated average  
 Nusselt number with  
 previous results

	$Gr$	This work	Petukhov <i>et al.</i> (1967/69)	Rustum and Soliman (1988)	Van Dyke (1990)	Mori <i>et al.</i> (1967)
$Pr = 7$	$10^4$	6.27	5.57	6.74	6.02	–
	$10^5$	8.43	8.43	8.58	8.18	–
$\alpha = 0^\circ \square$	$10^6$	10.64	12.75	11.87	11.13	–
	$10^5$	5.95	–	–	6.17	5.72
$Pr = 0.7$	$10^6$	7.87	–	–	8.24	8.43
	$10^7$	10.54	–	–	11.14	12.71
$Pr = 7$	$10^4$	4.44	4.46	–	–	–
	$10^5$	4.94	5.14	–	–	–
$\alpha = 0^\circ \square$	$10^6$	7.90	7.97	–	–	–



counter-rotating vortices. But for values of the Grashof number exceeding a critical value  $Gr_\ell$  the asymptotic state of the flows can change into a four-vortex structure.

Figure 2 shows the calculated flow and thermal characteristics of these two flow structures for  $Gr = 10^6$ ,  $Pr = 0.7$  and  $\alpha = 0^\circ$ . Despite the fact that the thermal boundary condition is different from that used by Nandakumar *et al.* (1985), the main characteristics of the two flow structures are qualitatively similar. Thus, for the two-vortex structure, the axial velocity and temperature distributions show a boundary layer behavior with pronounced radial gradients near the bottom of the cross-section. The secondary motion is particularly intense near the lower half of the interface. In the upper half of the cross-section the secondary velocities are very small and heat transfer takes place principally by conduction so that the isotherms are essentially parallel. It should be noted, however, that the vortex center is, in the present case, situated in the lower half of the cross-section, while for the conditions studied by Nandakumar *et al.* (1985) it was slightly above the horizontal diameter. On the other hand, the four-vortex solution is characterized by the presence of two additional symmetrical counter-rotating vortices in the lower part of the cross-section. This flow field no longer exhibits the boundary layer structure of the two-vortex solution and could therefore not be predicted by a boundary layer analysis such as that used by Siegwarth (1968). It is interesting to observe that the presence of the additional two vortices modifies considerably the axial velocity and temperature contours, especially in the lower part of the tube. Thus, the location of the maximum axial velocity clearly shifts upwards (Figure 3a). It should be noted that the value of this maximum is, for both flow structures, below the value of 2.0 corresponding to pure forced flow and that it is lower for the four-cell structure. Similarly, the temperature profile along the vertical diameter (Figure 3b) is significantly different between the two- and four-vortex solutions. The minimum temperature occurs closer to the tube axis and is not as low in the case of the four-vortex solution.

#### 4.1 Effects of the Grashof number

Figure 4 compares the structure of the flow and thermal fields corresponding to the four-vortex solution with water ( $Pr = 7.0$ ) in horizontal tubes for three different Grashof numbers. As the latter increases, the upper vortices decrease slightly in volume and move toward the lower wall. This behavior, which is attributed to the increase of natural convection effects, has also been observed in the case of the two-vortex solution (Siegwarth, 1968; Orfi, 1995). Concurrently, the lower cells move closer to the vertical diameter. Furthermore, as the Grashof number increases, the intensity of the secondary motion in both the upper and lower vortices increases. Thus, the corresponding extreme values of the stream function move further and further apart: they are (7.09, -4.81), (11.10, -7.69) and (21.5, -15.3) respectively for  $Gr = 2.5 \times 10^5$ ,  $10^6$  and  $10^7$ . It is also observed that despite the increase in the value of  $Gr$  the shape of the isotherms remains essentially unchanged, except for a very narrow region near

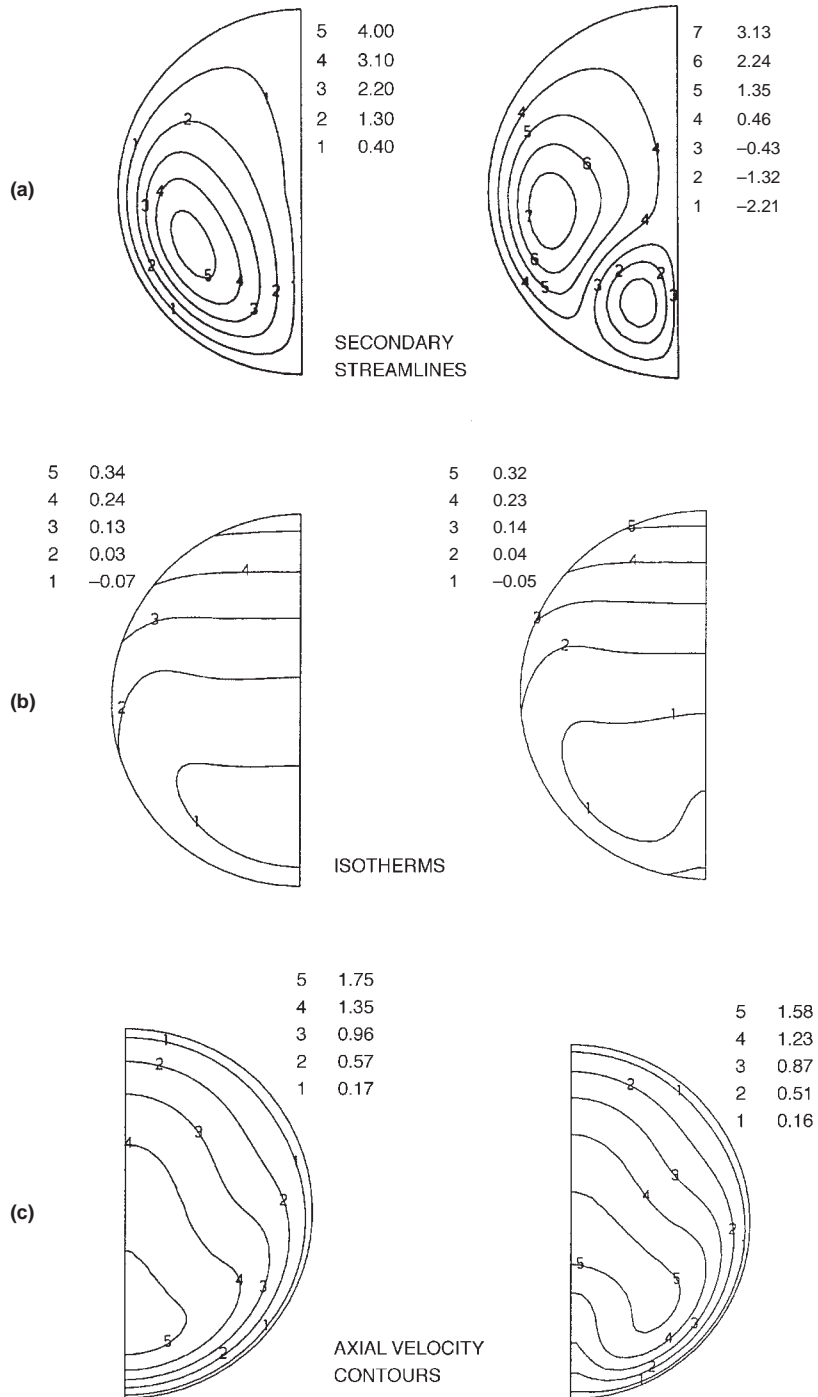


**Figure 2.**  
Dual solutions for  $Pr = 0.7$ ,  $Gr = 10^6$  and  $\alpha = 0^\circ$

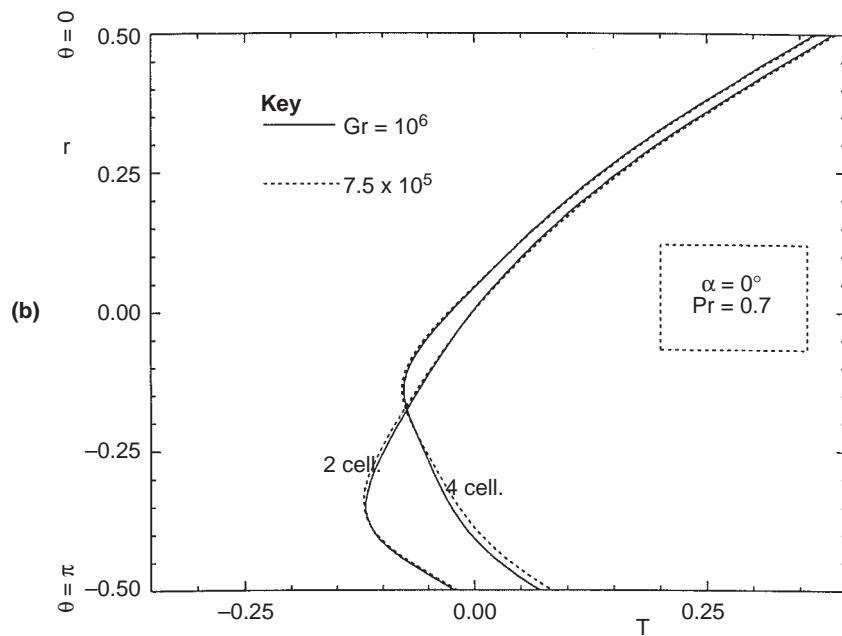
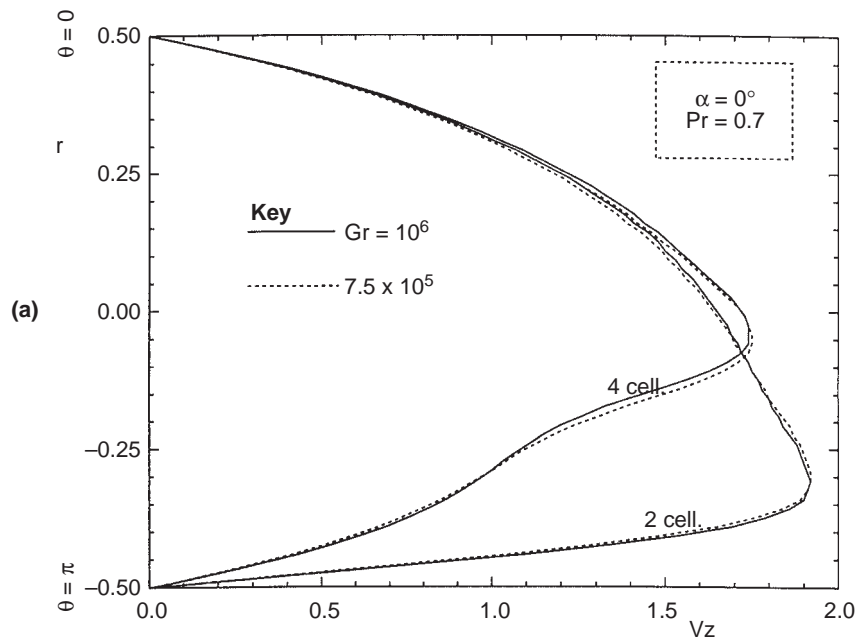


**Figure 3.**  
Axial velocity and  
temperature profiles  
along the vertical  
diameter

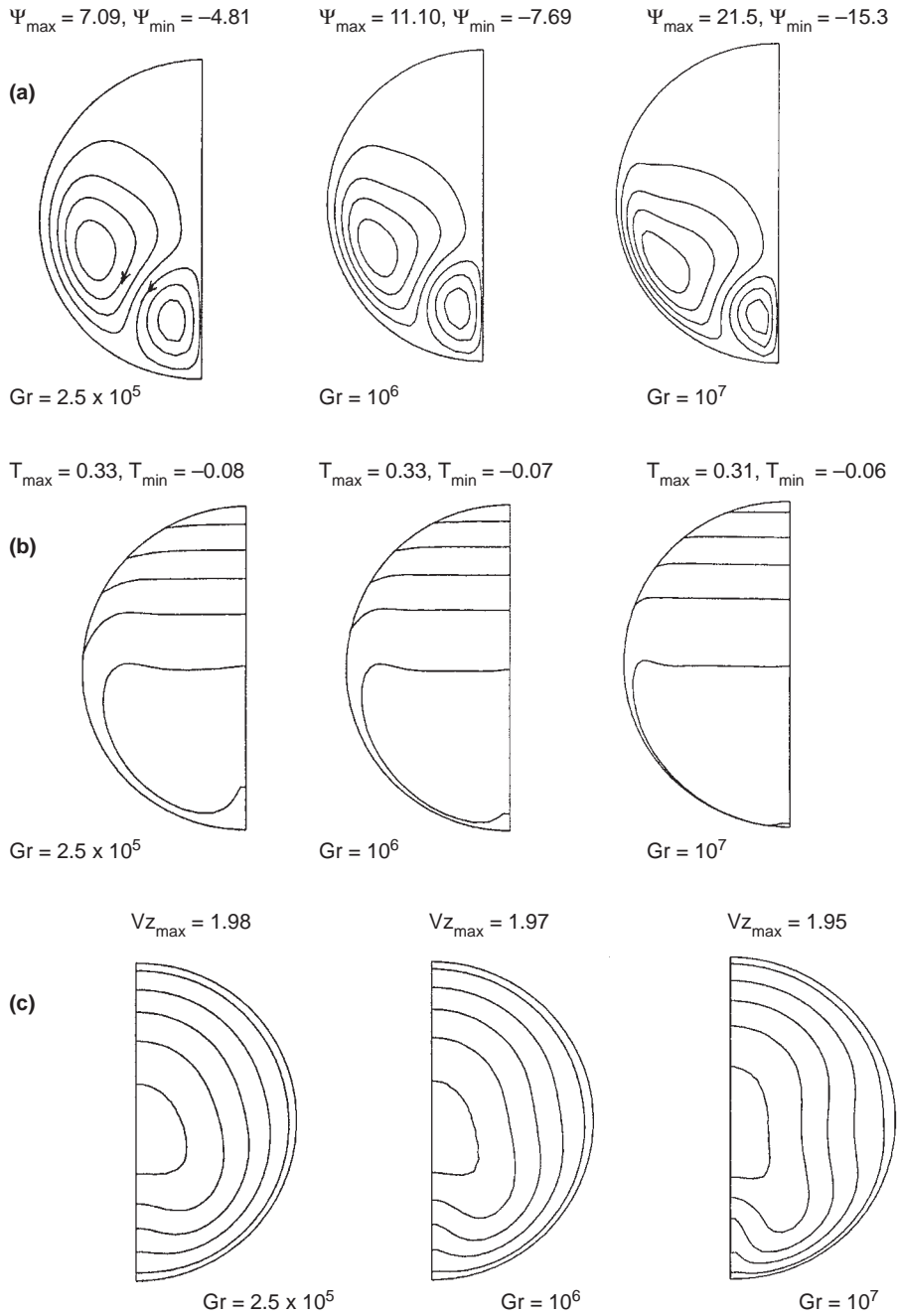


**Figure 4.** Effects of the Grashof on (a) the four-cell secondary flow structure, (b) the isotherms, and (c) the axial velocity field

the bottom of the tube. Regarding the axial velocity field it is noticed that the contours become more distorted, especially in the lower part of the tube where the new vortices are located, as the Grashof number increases. However, this axial field distortion appears to be less important than in the case of air (Figure 2) due to the higher viscosity of the water.

The wall shear stress and the Nusselt number variation with the Grashof number for both air ( $Pr = 0.7$ ) and water ( $Pr = 7.0$ ) are shown in Figure 5 (note that  $\tau_o = 8$  and  $Nu_o = 4.36$  are the values corresponding to pure forced flow). The flow bifurcation does indeed exist beyond a critical Grashof number,  $Gr_\ell$ . Thus for cases with low heating rates ( $Gr < Gr_\ell$ ) only the well-known two-vortex solution exists while for high heating rates ( $Gr > Gr_\ell$ ) the two-cell and four-cell solutions coexist. The results of this figure indicate that this critical Grashof number decreases with increasing Prandtl number. Thus,  $Gr_\ell$  has been determined to be approximately  $5.5 \times 10^5$ ,  $1.7 \times 10^5$  and  $1.7 \times 10^4$  respectively for  $Pr = 0.7$ , 7 and 70. This observation is consistent with similar behaviors established by Nandakumar *et al.* (1985) for both semi-circular and circular ducts, as well as by Nandakumar and Weinitschke (1991) for rectangular ducts. It can be explained by the fact that as  $Pr$  increases (i.e. as the fluid thermal diffusivity becomes relatively less important compared to its momentum diffusivity) the thermal boundary layer becomes thinner and the fluid temperature in the central part of the tube becomes more uniform. Therefore the secondary flow in this part of the tube is weakened with the increase of  $Pr$ . It therefore becomes less stable and more susceptible to convert from a two-cell to a four-cell structure.

It is also observed in Figure 5 that the circumferentially averaged wall friction and heat transfer coefficients for the four-cell structure are higher due to a more intense agitation of the fluid. However, the differences from the corresponding results of the two-cell solution are not significant. This behavior is qualitatively similar to that observed by Nandakumar *et al.* (1985) for a different thermal boundary condition.

Finally, it is important to explain the procedure used to obtain the dual solutions. The procedure which is normally employed (Nandakumar *et al.*, 1985; Choi and Choi, 1992) can be summarized as follows. Using the analytical solution for pure forced flow as the starting condition at the beginning of the iterative procedure, a two-vortex solution is obtained for a relatively low Grashof number, say  $Gr = 10^3$ . Then, using this two-vortex flow field as the new starting condition, a solution corresponding to a slightly higher Grashof number, say  $Gr = 5 \times 10^3$ , is computed. In this manner, flow fields with the two-cell structure can be obtained for ever increasing Grashof numbers. However, beyond a critical value  $Gr_u$  the two-cell structure is suddenly replaced by the four-cell one. On further increasing  $Gr$  beyond  $Gr_u$ , the four-cell flow structure can be maintained. Similarly, by gradually reducing  $Gr$  below  $Gr_u$ , the four-cell structure may persist until a second lower critical value  $Gr_\ell$  is reached. In this case, a hysteresis loop is present and dual solutions exist for  $Gr_u > Gr > Gr_\ell$ .

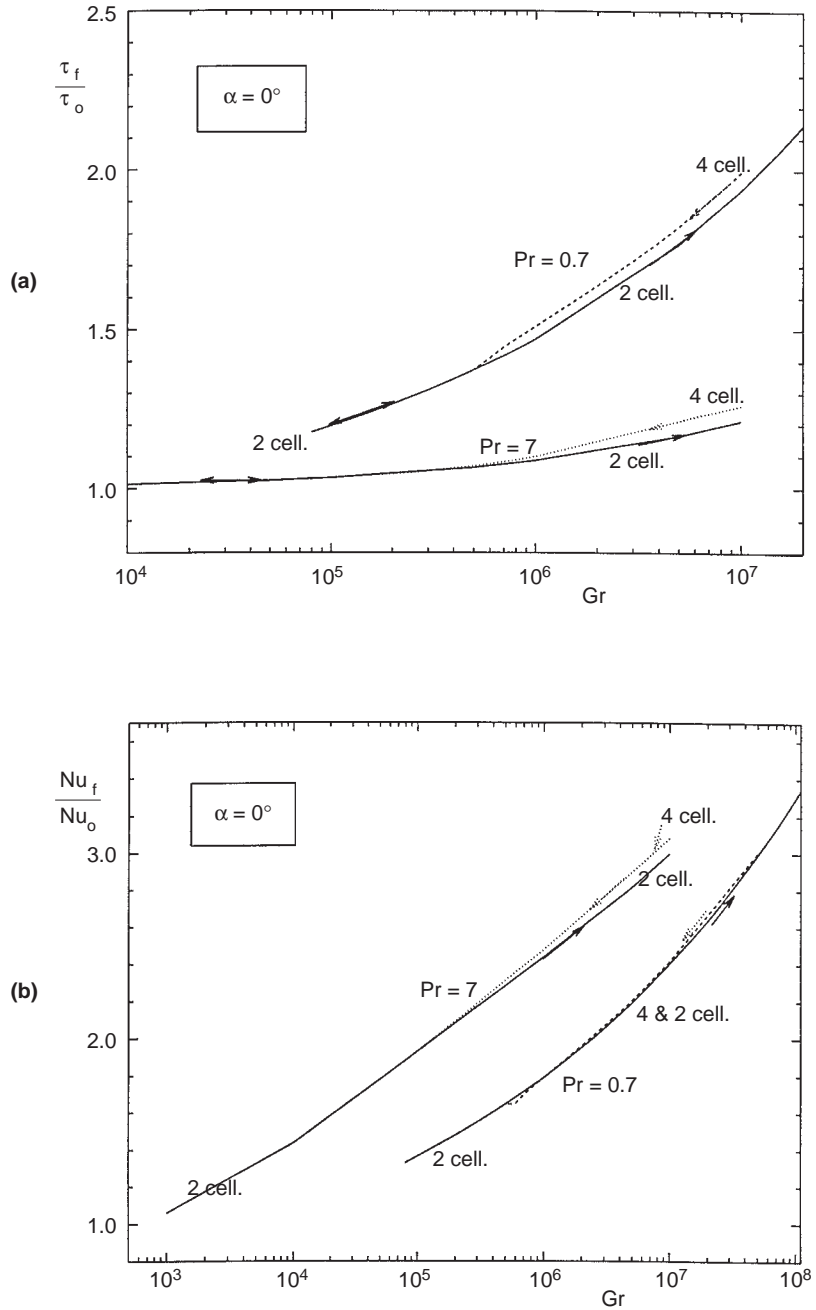


**Figure 5.** Effect of  $Gr$  on the circumferentially averaged values of (a) the wall shear stress, and (b) the Nusselt number

With regard to the results of Figure 5, it can be seen that only the lower critical Grashof number  $Gr_\ell$  was obtained and that the hysteresis loop was not detected. As the upper critical Grashof value  $Gr_u$  was not reached, the four-vortex solution could not be established as a unique flow structure. In order to trigger such a solution for air in a horizontal tube at some high Grashof number, say  $Gr = 10^7$ , we used the pure forced flow solution as the starting condition at the beginning of the iterative procedure for that particular Grashof number. This approach led to a four-vortex converged solution which could then be used as an initial guess leading to four-cell structures for slightly different sets of the three controlling parameters  $Pr$ ,  $Gr$  and  $\alpha$ .

#### 4.2 Effect of the tube inclination

The presence of a buoyancy force component along the axial direction complicates the mixed convection flow field. For the two-vortex solution it has been reported that the maximum axial velocity occurs below the tube axis for horizontal (Figure 3a) and nearly horizontal tubes while in the case of steeply inclined tubes this maximum may be located well above the axis (Orfi *et al.*, 1993; Orfi, 1995). Furthermore, the local wall shear stress varies considerably along the tube perimeter. For horizontal tubes, the product  $\tau \cdot Re$  is more important in the lower part of the wall while for steeply inclined tubes the reverse has been observed. In general, the circumferentially averaged value of the product  $\tau \cdot Re$  increases appreciably with increasing tube inclination (Orfi *et al.*, 1993). In this section, the effects of the tube inclination on the flow bifurcation will be discussed. To the authors' knowledge, these effects have not been reported in the literature for any thermal boundary condition.

Figure 6 shows the secondary flow patterns corresponding to the two- and four-vortex structures for  $Pr = 7$ ,  $Gr = 10^6$  and four different tube inclinations. It is observed that, for the two-cell structure, the intensity of the buoyancy-induced secondary motion changes significantly with  $\alpha$ . In fact, based on the maximum value of the stream function this secondary motion reaches a maximum intensity for a tube inclination close to  $40^\circ$  (see also discussion by Orfi *et al.* (1993)). The position of the vortex center moves slightly upwards and away from the tube wall as  $\alpha$  increases. For  $\alpha = 80^\circ$ , the flow field is nearly symmetrical with respect to the horizontal diameter  $\theta = -\pi/2, \pi/2$ . In the case of the four-vortex structure, we notice once again that – based on the difference between the extreme values of the stream function – the secondary motion intensity is maximum for a tube inclination close to  $40^\circ$ . The lower cells increase slightly with an increase of the tube inclination, thus forcing the upper cells to move upwards.

The influence of the tube inclination on the thermal field and on the axial velocity contours for the four-vortex structure is illustrated in Figure 7. It is observed that thermal stratification, expressed by the difference between the extreme fluid temperatures, decreases with an increase in  $\alpha$ . This behavior, which results from the decrease of the cross-sectional effects of buoyancy with increasing tube inclination, is similar to that observed by Orfi *et al.* (1993) for

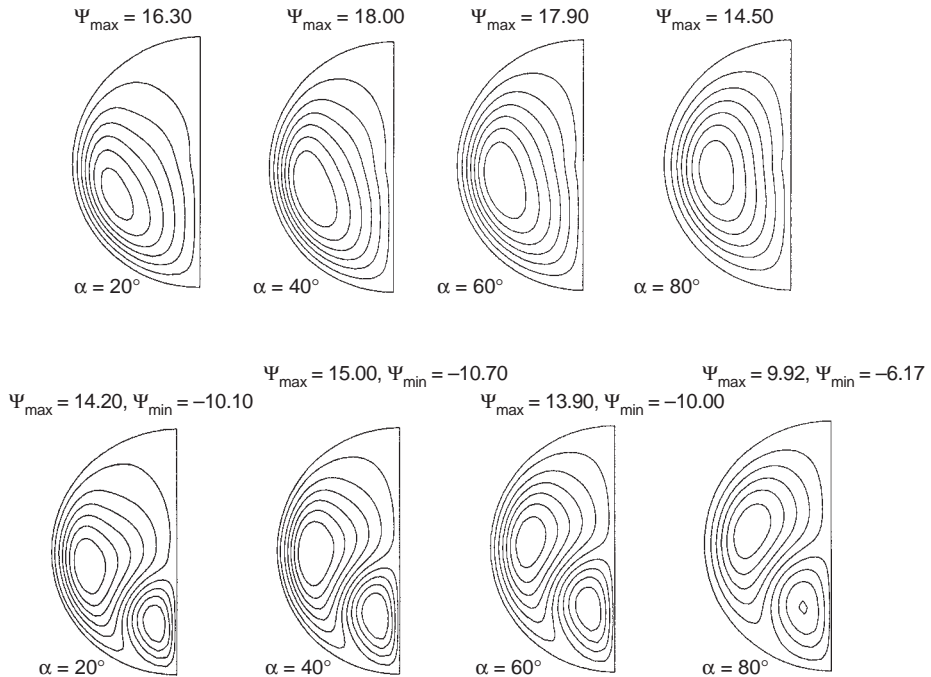


**Figure 6.**  
Dual solutions for  $Pr = 7$ ,  $Gr = 10^6$  and  $\alpha = 20^\circ$ ,  $40^\circ$ ,  $60^\circ$  and  $80^\circ$

the two-vortex structure. Owing to the increase in size of the lower cells, the isotherms become very distorted in the lower part of the tube, in particular for steeply inclined tubes. From Figure 7, it can also be observed that, in contrast to the case of horizontal tubes, the region of high axial velocities is located above the horizontal diameter. In fact, the position of the maximum axial velocity moves upwards as  $\alpha$  increases. This tendency results from the effects of the buoyancy force, which has components in both the axial and transverse directions for inclined tubes. The same tendency has also been reported previously for the two-vortex structure by Orfi *et al.* (1993) and by Laouadi *et al.* (1994).

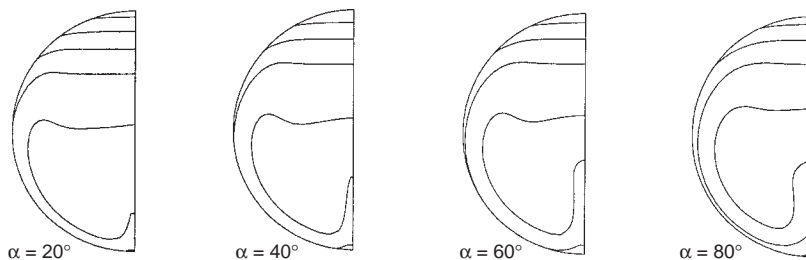
It should be pointed out that for a vertical tube the calculated flow field, which is not reproduced here, is independent of the angular coordinate  $\theta$ . For this particular inclination the radial and tangential velocity components are zero and, therefore, there is no motion in a cross-section perpendicular to the tube axis.

Figure 8 shows the angular variation of the local Nusselt number for the two flow structures and different tube inclinations. It is observed that over a large part of the wall (for  $\theta$  between 0 and approximately 2.4) the local heat transfer coefficient increases with  $\theta$  and is essentially not influenced by the flow structure. For  $\theta > 2.4$ , however,  $Nu_\theta$  for the four-vortex structure is considerably lower than that for the two-vortex structure. This behavior is due to the effect of the counter-



ISOTHERMS

$T_{\max} = 0.23, T_{\min} = -0.05$     $T_{\max} = 0.20, T_{\min} = -0.05$     $T_{\max} = 0.18, T_{\min} = -0.05$     $T_{\max} = 0.17, T_{\min} = -0.05$



AXIAL VELOCITY CONTOURS

$V_{z_{\max}} = 2.17$     $V_{z_{\max}} = 2.48$     $V_{z_{\max}} = 2.69$     $V_{z_{\max}} = 2.79$

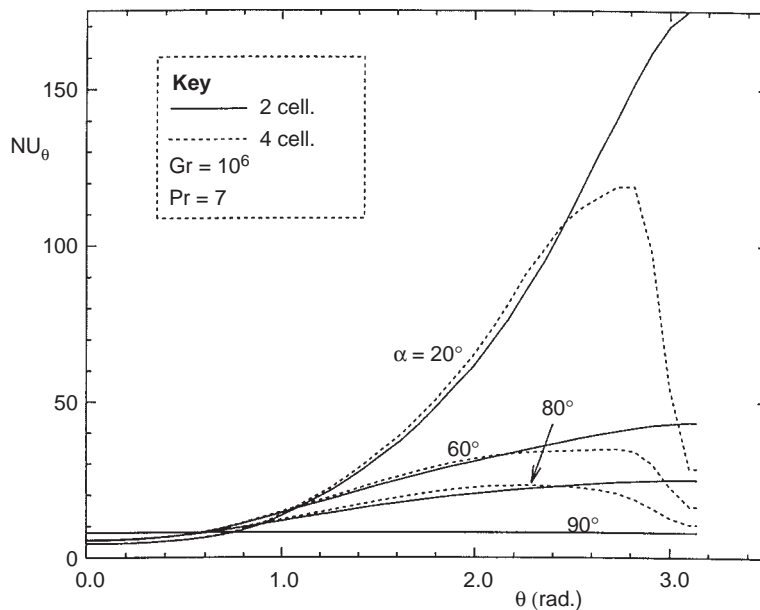
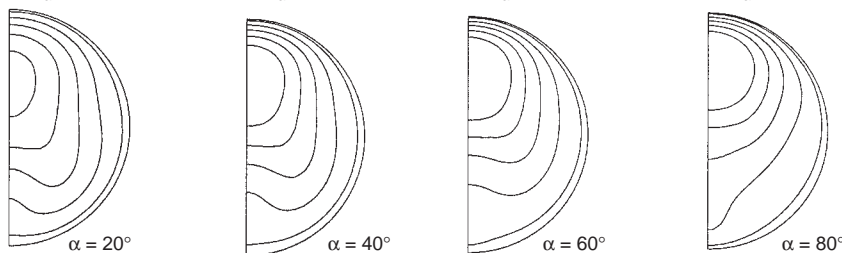


**Figure 8.**  
Circumferential distribution of the local Nusselt number for two- and four-vortex solutions

**Figure 7.**  
Isotherms and axial velocity fields for the four-cell solutions of Figure 6

rotating lower eddies which move cold fluid from the central region towards the cold bottom part of the tube. Thus, for inclined tubes, the two-vortex structure provides an improved heat transfer performance.

Further information concerning the effects of flow bifurcation with respect to the tube inclination is provided in Figures 9 and 10. Figure 9a, which shows the variation of the circumferentially averaged wall shear stress with  $\alpha$ , indicates that the four-cell structure results in slightly higher flow resistance. Figure 9b, which shows the variation of the similarly averaged Nusselt number, shows that the influence of flow structure on this parameter is not particularly important. On the other hand, Figures 10a for water and 10b for air, showing the axial velocity along the tube axis as a function of tube inclination, indicate that this velocity is significantly influenced by the secondary flow structure. However, the most important information in Figures 9 and 10 is the fact that dual solutions exist only for  $\alpha$  between  $0^\circ$  and a critical value  $\alpha_c$ . Above  $\alpha_c$ , only the two-vortex solution has been obtained. This critical tube inclination depends strongly on the Prandtl number. Thus, for the Grashof number under consideration ( $Gr = 10^6$ )  $\alpha_c$  is situated within the intervals ( $62^\circ, 63^\circ$ ) and ( $83^\circ, 84^\circ$ ) for air and water respectively. It is interesting to notice that the range of angle inclinations with a unique solution (two-vortex in this case) decreases as the Prandtl number increases due to the decrease in the thickness of the thermal boundary layer mentioned earlier.

#### 4.3 Effects of the Prandtl number

The effects of  $Pr$  on the flow structure are examined in Figure 11, which shows the variation of the axial fluid velocity along the tube axis for  $Gr = 10^6$  and two tube inclinations. It is observed that dual solutions coexist for both tube inclinations over the entire range of Prandtl values considered. It should be noted that for the high heating rate under consideration and for  $\alpha = 60^\circ$  the calculated value for the two-cell structure is higher than 2.0, which is the corresponding value for pure forced flow.

The influence of the Prandtl on the circumferentially averaged Nusselt number and wall shear stress is illustrated in Figure 12 for  $\alpha = 0^\circ$  and  $\alpha = 60^\circ$ . An increase of  $Pr$  results in an appreciable enhancement of the heat transfer coefficient, in particular for steeply inclined tubes. For horizontal tubes this effect is less important. This behavior can be explained by noting that for horizontal flows the temperature stratification in the upper part of the tube is very important, especially for high Grashof numbers. The difference between the results corresponding to two- or four-vortex structures is more significant for  $\alpha = 60^\circ$ . Concerning the effect of  $Pr$  on the wall shear stress (Figure 12b) it is observed that the latter decreases as  $Pr$  increases. Once again the difference associated with the secondary flow structure is more important for  $\alpha = 60^\circ$ .

The arrows on the curves of Figures 11 and 12 indicate that the solutions for the two-vortex structure were obtained by gradually increasing the Prandtl number, while those for the four-vortex structure were obtained by gradually

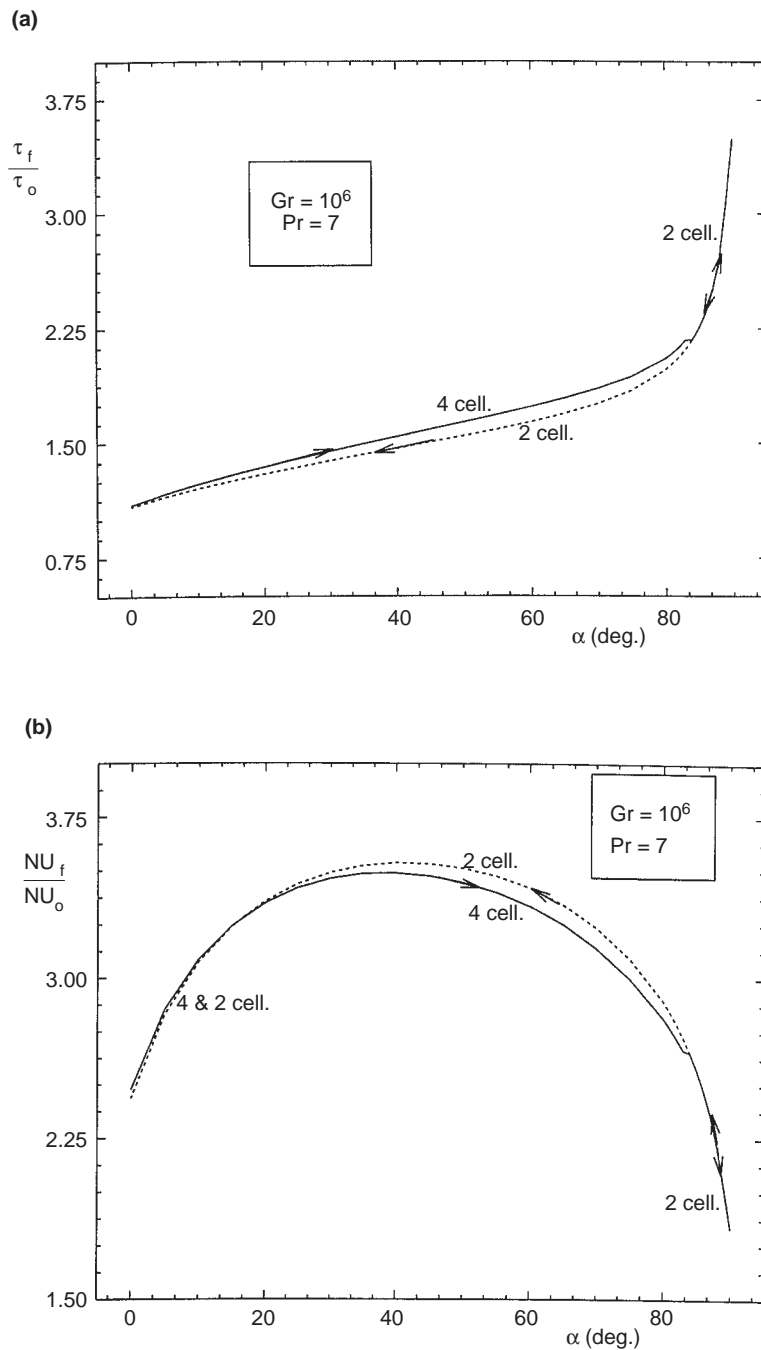


**Figure 9.**  
Effect of  $\alpha$  on the circumferentially averaged values of (a) the wall shear stress, and (b) the Nusselt number

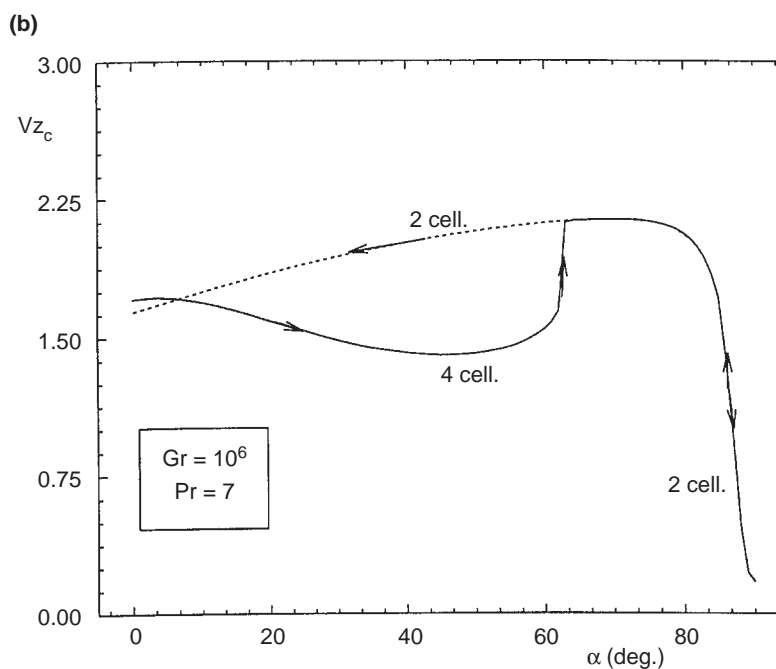
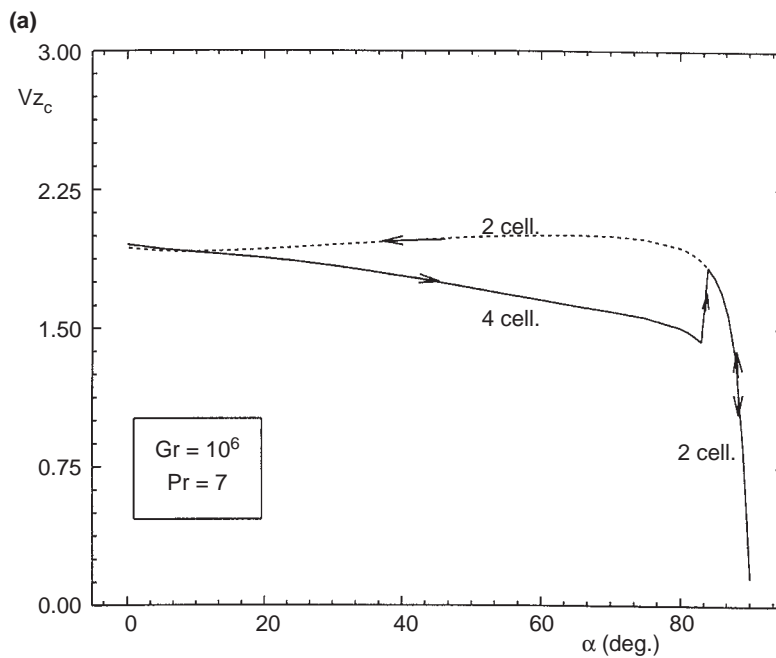


**Figure 10.**  
Effect of  $\alpha$  on the axial  
velocity along the  
centerline for (a) water,  
and (b) air

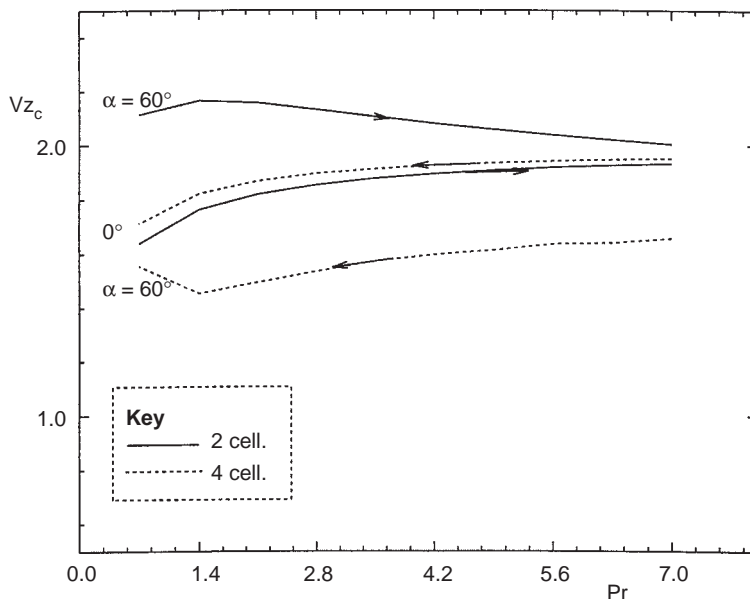


**Figure 11.**  
State diagram for the axial velocity along the centerline as a function of  $Pr$

decreasing it. This procedure was used in an unsuccessful attempt to detect the existence of upper or lower critical values of  $Pr$  beyond which only one of these two secondary flow structures would exist.

## 5. Evaluations and discussion of results

As already mentioned, the results presented in the previous section were calculated based on the assumption of fully developed flow (i.e. using the conditions expressed by equations (2)). In order to better understand the phenomenon of flow bifurcation, we have also attempted to determine whether it could occur in a developing flow. In other words, we were interested to investigate how the secondary flow evolved in the entrance region of the tube and whether, for example, the four-vortex structure always occurred after transition from a two-vortex one. For this purpose we have considered the problem of the hydrodynamically and thermally developing laminar mixed convection flow in inclined tubes subject to a uniform heat flux condition at the wall-fluid interface. The axial velocity and temperature profiles were assumed uniform at the tube inlet ( $Z = 0$ ) and the condition of symmetry about the vertical diameter was also used.

A modified version of the Patankar-Spalding method for three-dimensional axially parabolic flows (Orfi *et al.*, 1994; Orfi, 1995) was then used to calculate the developing temperature and velocity fields for many different combinations of the four governing parameters. The calculations were carried out over a tube length sufficient to attain fully developed flow conditions. All the results thus calculated correspond to a two-vortex secondary flow structure (Orfi *et al.*, 1997). We even tried to perturb the developing flow field by imposing a four-

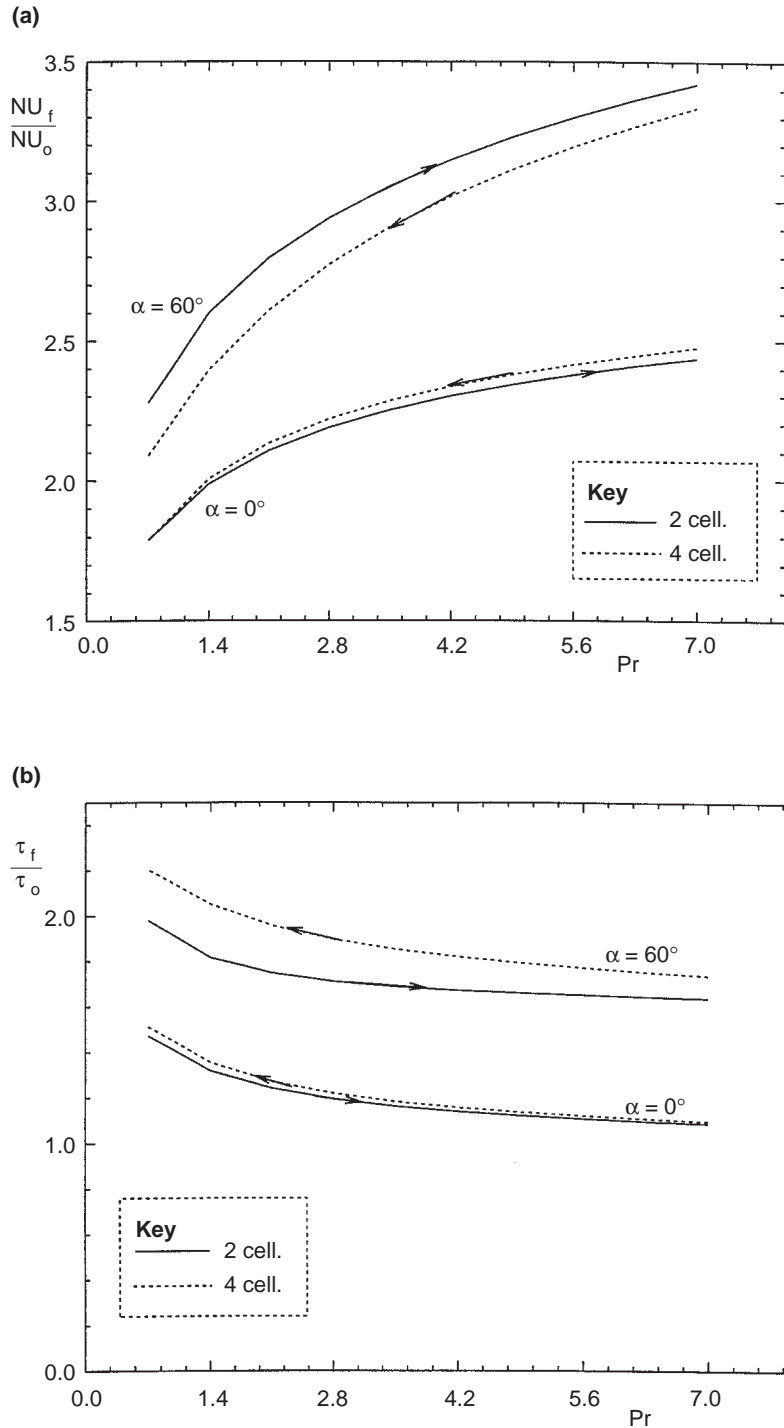


**Figure 12.**  
Effect of  $Pr$  on the  
circumferentially  
averaged values of (a)  
the Nusselt number, and  
(b) the wall shear stress

vortex solution at every axial cross-section in the entrance region of the tube. This imposed four-vortex solution corresponds to the fully developed flow of air at  $Gr = 10^6$  in a horizontal tube. However, this perturbation did not have any influence on the resulting secondary flow structure after convergence. The two-vortex structure was consistently recovered and we were never able to obtain the four-vortex solution after convergence. This interesting behavior of the solution, i.e. convergence to the two-vortex solution after being perturbed, indicates that the two-cell structure is the only stable flow structure.

This last conclusion is supported by experimental evidence. So far all experimental investigations have confirmed the existence of the two-vortex flow structure. To the best of our knowledge, there is no experimental evidence for the existence of the four-vortex flow structure for the problem studied here. In fact, such an experimental confirmation cannot be based on the most commonly reported data which concern the circumferentially averaged Nusselt number since this parameter does not vary much with the secondary flow structure. The only easily measured variables which are significantly influenced by this flow structure are the axial velocity and temperature profiles for tube inclinations below the critical angle  $\alpha_c$  (see Figures 3, 10 and 11). However, since very few experimental studies report such profiles and no one has specifically studied this issue experimentally for mixed convection, it is impossible to dismiss the four-vortex structure as a physically possible secondary flow field for such flows. Indeed, by analogy to other flows with well documented bifurcation characteristics (such as the Taylor and Dean problems) such a structure for the present problem must be accepted as plausible.

## 6. Conclusions

The problem of bifurcation for fully developed laminar mixed convection of a Boussinesq fluid within inclined tubes subject to a uniform wall heat flux has been investigated numerically with respect to the tube inclination  $\alpha$ , the Grashof number  $Gr$  and the Prandtl number  $Pr$ . Dual solutions with a two- and four-vortex secondary flow structure in a cross-section normal to the tube axis have been found for different combinations of  $\alpha$  and  $Gr$  for all Prandtl numbers between 0.7 and 7. State diagrams for the axial velocity and temperature indicate that these variables are considerably influenced by the secondary flow structure. On the other hand, global quantities such as the circumferentially averaged Nusselt number and wall shear stress are essentially insensitive to the secondary flow structure.

For relatively low heating rates (i.e. for  $Gr$  below a critical value  $Gr_\ell$  which increases with decreasing  $Pr$ ) and for steeply inclined tubes (i.e. for tube inclinations above a critical value  $\alpha_c$  which increases with increasing  $Pr$ ) only the two-vortex solution exists. Numerical experiments carried out for developing flows indicate that the two-vortex structure is the only stable solution.

**References**

- Bara, B., Nandakumar, K. and Masliyah, J.H. (1992), "An experimental and numerical study of the Dean problem: flow development towards two-dimensional multiple solutions", *J. Fluid Mech.*, Vol. 244, pp. 339-76.
- Barozzi, G.S. *et al.* (1985), "Experimental investigation of combined forced and free convection in horizontal and inclined tubes", *Meccanica*, Vol. 20 No 1, pp. 18-27.
- Benjamin, T.B. (1978a), "Bifurcation phenomena in steady flows of a viscous fluid, I. Theory", *Proc. R. Soc. Lon.*, A.359, pp. 1-26.
- Benjamin, T.B. (1978b), "Bifurcation phenomena in steady flows of a viscous fluid, II. Experiments", *Proc. R. Soc. Lon.*, A.359, pp. 27-43.
- Benjamin, T.B. and Mullin, T. (1982), "Notes on the multiplicity of flows in the Taylor experiment", *J. Fluid Mech.*, Vol. 121, pp. 219-30.
- Bilodeau, S., Galanis, N. and Laneville, A. (1997), "Transition dans un conduit cylindrique soumis à un flux de chaleur uniforme à la paroi", *Actes du Congrès de la Société Française des Thermiciens*, Toulouse, France, pp. 215-18.
- Choi, D.K. and Choi, D.H. (1992), "Dual solution for mixed convection in a horizontal tube under circumferentially non-uniform heating", *Int. J. Heat Mass Transfer*, Vol. 35 No. 8, pp. 2053-6.
- Chou, F.C. and Hwang, G.J. (1984), "Flow visualization studies on secondary flow patterns in straight tubes downstream of a 180° bend and in isothermally heated horizontal tubes", *Trans. ASME: J. Heat Transfer*, Vol. 109, pp. 49-54.
- Choudhury, D. and Patankar, S.V. (1988), "Combined forced and free laminar convection in the entrance region of an inclined isothermal tube", *Trans. ASME: J. Heat Transfer*, Vol. 110, pp. 901-8.
- Collins, M.W. (1971), "Combined convection in vertical tubes, heat and mass transfer by combined forced and natural convection", *Proc. Inst. Mech. Engrs. Symp.*, University of Manchester, Owens Park, UK, Paper No. C115-71, pp. 17-25.
- Coutier, J.P. (1983), "Laminar convection with buoyancy in tube flows with a surrounding liquid medium", PhD thesis, University of California, Berkeley, CA.
- Heggs, P.J., Ingham, D.B. and Keen, D.J. (1990), "The effects of heat conduction in the wall on the development of recirculating combined convection flows in vertical tubes", *Int. J. Heat Mass Transfer*, Vol. 33, pp. 517-28.
- Kakac *et al.* (1987), *Handbook of Single-phase Convective Heat Transfer*, John Wiley & Sons, New York, NY.
- Laouadi, A., Galanis, N. and Nguyen, C.T. (1994), "Laminar fully developed mixed convection in inclined tubes uniformly heated on their outer surface", *Num. Heat Transfer*, Part A., Vol. 26, pp 719-38.
- Morcós, S.M. (1974), "Combined forced and free laminar convection in horizontal tubes", PhD thesis, Iowa State University.
- Mori, Y., Futagami, K. *et al.* (1967), "Forced convective heat transfer in uniformly heated horizontal tubes, 1st report, experimental study", *Int. J. Heat Mass Transfer*, Vol. 9, pp. 453-63.
- Morton, B.R. (1959), "Laminar convection in uniformly heated horizontal pipes at low Rayleigh number", *Quart. J. Mech. Appl. Math.*, Vol. 12, pp. 401-20.
- Nandakumar, K. and Masliyah, J.H. (1982), "Bifurcation in steady laminar flow through curved tubes", *J. Fluid Mech.*, Vol. 119, pp. 475-90.
- Nandakumar, K. and Weinitschke, H.J. (1991), "A bifurcation study of mixed convection heat transfer in horizontal ducts", *J. Fluid Mech.*, Vol. 231, pp. 157-87.



- Nandakumar, K., Masliyah, J.H. and Law, H.S. (1985), "Bifurcation in steady laminar mixed convection flow in horizontal ducts", *J. Fluid Mech.*, Vol. 152, pp. 145-61.
- Nesreddine, H., Galanis, N. and Nguyen, C.T. (1997), "Variable-property effects in laminar aiding and opposing mixed convection of air in vertical tubes", *Num. Heat Transfer*, pt. A, Vol. 31, pp. 53-69.
- Newel, P. and Bergles, A.E. (1970), "Analysis of combined free and forced convection for fully-developed laminar flow in horizontal tubes", *J. Heat Transfer*, Vol. 92 No. 1, pp. 83-93.
- Orfi, J. (1995), "Convection mixte laminaire dans un tuyau incliné: développement simultané et phénomène de bifurcation", PhD thesis, Université de Sherbrooke, Canada, p. 166.
- Orfi, J., Galanis, N. and Nguyen, C.T. (1993), "Laminar fully developed incompressible flow with mixed convection in inclined tubes", *Int. J. of Numerical Methods for Heat & Fluid Flow*, Vol. 3 No. 4, pp. 341-55.
- Orfi, J., Galanis, N. and Nguyen, C.T. (1994), "Laminar mixed convection flow in the entrance region of uniformly heated inclined tubes", in Wrobel, L.C., Brebbia C.A. and Nowak, A.J. (Eds), *Advanced Comp. Meth. Heat Transfer III*, Comp. Mech. Publications, pp. 45-52.
- Orfi, J., Galanis, N. and Nguyen, C.T. (1997), "Développement simultané hydrodynamique et thermique d'un écoulement laminaire dans un tube incliné en régime de convection mixte", *Revue Gén. Thermique*, Vol. 36, pp. 83-92.
- Patankar, S.V. (1980), *Numerical Heat Transfer and Fluid Flow*, Hemisphere Publishing Corporation and McGraw-Hill Book Company, New York, NY.
- Patankar, S.V., Ramadhyani, S. and Sparrow, S. (1978), "Effect of circumferentially non-uniform heating on laminar combined convection in a horizontal tube", *Trans. ASME : J. Heat Transfer*, Vol. 100, pp. 63-70.
- Petukhov, B.S. and Polyakov, A.F. (1967), "Experimental investigation of visco-gravitational fluid flow in a horizontal tube", *Sci. Res. Inst. of High Temp.*, Vol. 5 No. 1, pp. 87-95.
- Petukhov, B.S. *et al.* (1969), "Heat transfer in tubes with viscous-gravity flow", *Heat Transfer Soviet Research*, Vol. 1 No 1, pp. 34-31.
- Siegwarth, D.B. (1968), "Effect of free convection on laminar flow through a horizontal pipe", PhD thesis, University of Illinois, Urbana, p. 182.
- Van Doormal, J.P. and Raithby, G.D. (1984), "Enhancements of the SIMPLE method for predicting incompressible fluid flows", *Num. Heat Transfer*, Vol. 7, pp. 147-63.
- Van Dyke, M. (1990), "Extended Stokes series: laminar flow through a heated horizontal pipe", *J. Fluid Mech.*, Vol. 212, pp. 289-308.
- Wang, M., Tsuji, T. and Nagano, Y. (1994), "Mixed convection with flow reversal in the thermal entrance region of horizontal and vertical pipes", *Int. J. Heat Mass Transfer*, Vol. 37, pp. 2305-19.
- Winters, K.H. (1987), "A bifurcation study of laminar flow in a curved tube of rectangular cross-section", *J. Fluid Mech.*, Vol. 180, pp. 343-69.

### Further reading

- Rustum, I.M. and Soliman, H.M. (1988), "Experimental investigation of laminar mixed convection in tubes with longitudinal internal fins", *J. Heat Transfer*, Vol. 110, pp. 366-72.